Optical Engineering

SPIEDigitalLibrary.org/oe

Dynamic temperature field measurements using a polarization phase-shifting technique

David Ignacio Serrano-García
Amalia Martínez-García
Noel-Ivan Toto-Arellano
Yukitoshi Otani

SPIE

Dynamic temperature field measurements using a polarization phase-shifting technique

David Ignacio Serrano-García,[a,b,*] Amalia Martínez-García,[a] Noel-Ivan Toto-Arellano,[c] and Yukitoshi Otani[b]
[a]Centro de Investigaciones en Óptica A.C., León, Gto., México
[b]Utsunomiya University, Center of Optical Research and Education, 7-1-2 Yoto, Utsunomiya, Tochigi 321-8585, Japan
[c]Laboratorio de Óptica y Fotónica de la Universidad Tecnológica de Tulancingo, Tulancingo, Hidalgo, México

Abstract. In this study, an optical system capable of simultaneously grabbing three phase-shifted interferometric images was developed for dynamic temperature field measurements of a thin flame. The polarization phase-shifting technique and a Michelson interferometer that is coupled to a 4-*f* system with a Ronchi grating placed at the frequency plane are used. This configuration permits the phase-shifted interferograms to be grabbed simultaneously by one CCD. The temperature field measurement is based on measuring the refraction index difference by solving the inverse Abel transform, which requires information obtained by the fringe order localization. The phase map is retrieved by a three-step algorithm. Experimental results of a dynamic thin flame are presented. [DOI: 10.1117/1.OE.53.11.112202]

Keywords: interferometry; polarization; phase shifts; temperature; diffraction.

Paper 131460SS received Sep. 23, 2013; revised manuscript received Dec. 19, 2013; accepted for publication Dec. 30, 2013; published online Feb. 28, 2014.

1 Introduction

In phase-shifting techniques, a stepping motor or piezoelectric transducers are normally used to move a reference surface to get the interference fringe images with a relative phase shift. However, this takes a period of time, making it susceptible to environmental effects such as ambient vibration or air turbulence, which results in measurement errors. To facilitate the applicability of interferometric techniques for measuring dynamic events, a system that is capable of acquiring several phase-shifted images instantaneously or simultaneously is required. As a result of this capability, a reduction of environmental disturbances is encountered, increasing the accuracy and stabilization of the system.

In this study, a measurement system that is capable of grabbing three phase-shifted interferometric images instantaneously (or simultaneously) was developed for dynamic temperature measurement over a period of time. The system presented is based on polarization phase-shifting techniques presented previously,[1–3] with the addition of calibration procedures and digital fringe processing techniques in order to accurately measure temperature fields varying in time.

Single-shot polarization phase-shifting techniques are currently a focus field of study, and the most important and an industry standard nowadays are pixelated phase mask interferometers. One of the principal properties of these systems is that the modulating phase-mask remains fixed, placed before the CCD light sensor.[4] Nowadays, some authors present novel algorithms based on this property; for example, in the demodulation form, algorithms focused on harmonics rejections, and recently encountered more accurate results by proposing an extension of the phase-shifting unit cell.[5,6]

Other single-shot systems are based on the use of a three-layer sensor to detect three wavelengths; these systems have been applied accurately by fringe projections profilometry[7] and digital holographic system.[8] Interferometric polarization phase-shifting techniques also have been employed before in different techniques; some of them are based on using Wollaston prisms and polarization gratings[9] by using a prism and a glass plate with different thicknesses,[10] and lately a system capable of acting as a fringe projection system, or a shearing interferometer by employing a Savart plate and liquid crystals.[11]

Alternative systems, also based on phase-shifting polarization techniques, have been presented before.[2,12] These systems are based on obtaining interference replicas by using phase/amplitude gratings,[12] and also they only retrieve the phase data map. The interferogram amplitude modulation change obtained by the replication system was solved earlier by using two crossed gratings and selecting the orders with equal amplitude.[2,3,12] Even this amplitude modulation change was minimum when using phase gratings,[3,12] it was still encountered. In this work, the selection of an amplitude grating is to emphasize the amplitude modulation change and how this can be solved by a fringe normalization process.

In order to implement a system capable of obtaining temperature field measurements of a flame varying in time, we implemented calibration and normalization procedures.

In this work, the temperature field measurement is based on measuring the refraction index difference by solving the inverse Abel transform. The inversion of the Abel transform is solved with the information obtained by the fringe order localization of the deformed fringe pattern generated by the flame under study.

This paper is organized in five sections, including the present introduction. Section 2 discusses the theoretical background of the single-shot procedure by first explaining the phase data map retrieval and then the relationship with

*Address all correspondence to: David Ignacio Serrano-García, E-mail: david@cio.mx

the temperature field measurement. In Sec. 3, the experimental setup is described, and the dynamic temperature field measurements are presented. Finally, in Sec. 4, conclusions are presented.

2 Temperature Fields Measurements by Means of Phase Data Map Calculation

Interference occurs when placing a quarter-wave plate and a linear polarizer at the output of an interferometer that has its reference and object beams with orthogonal linear polarization. Interference is between the right-handed and left-handed circularly polarized states in objects and reference beam, respectively. A desired phase shift will be obtained and controlled by the angle of the polarizer.[13,14] This consideration is suitable in the implementation for a single-shot phase-shifting interferometer.

The optical setup presented for the optical phase calculation consists of a polarization Michelson interferometer (PMI) that is coupled to a 4-f system with an amplitude grating placed at the Fourier plane (Fig. 1). As a result, the interferogram first obtained by the PMI is replicated at the image plane of the 4-f system (Fig. 2).

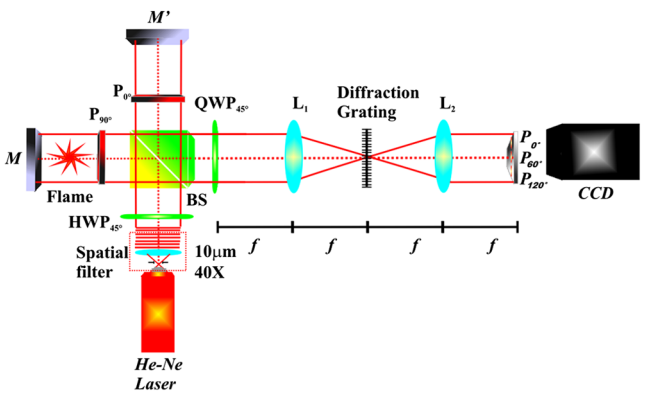

Fig. 1 Setup of the instantaneous polarized phase-shifting interferometer. The polarizing Michelson interferometer (PMI) is coupled to a 4-*f* system in order to obtain replicas of the interference pattern at the output. Each interferogram retrieved presents a relative phase shift of 120 deg. Mirror: M; half wave plate: HWP; lens: Li; polarizers: Pi; quarter wave plate: QWP; beam splitter: BS.

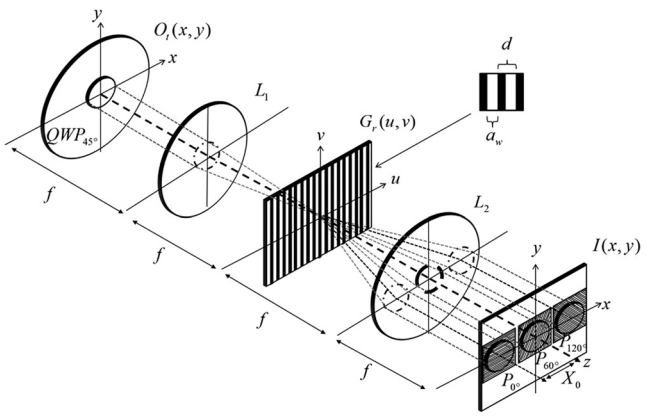

Fig. 2 Interferogram replication system based on a 4-*f* system with an amplitude grating in the Fourier plane. The necessary phase shifted interferograms are captured in the same image.

2.1 *Polarization Phase Shifting Technique*

The output beam of the interferometer, after passing the quarter-wave plate, can be represented as the sum of the states, object and reference beam, with circular polarization states in opposite directions, respectively

$$O_t(x,y) = \frac{1}{\sqrt{2}}\begin{pmatrix}1\\ i\end{pmatrix}e^{-i\varphi(x,y)} + \frac{1}{\sqrt{2}}\begin{pmatrix}1\\ -i\end{pmatrix}, \tag{1}$$

when this field is observed through a linear polarizing filter P_θ whose transmission axis is at angle θ

$$\mathbf{P_\theta} = \begin{bmatrix}\cos^2\theta & \sin\theta\cos\theta\\ \sin\theta\cos\theta & \sin^2\theta\end{bmatrix}. \tag{2}$$

The resulting irradiance is associated with the interference pattern with a phase shift introduced twice the angle of the polarizers.

$$I_\theta(x,y) = |\mathbf{P_\theta}\cdot O_t|^2 = 1+\cos[\varphi(x,y)+2\theta]. \tag{3}$$

2.2 *Interferogram Pattern Replication*

The transmittance of a Ronchi grating of spatial period $d = (\lambda f)/(X_0)$ that is placed in the Fourier Plane can be written as

$$\begin{aligned} G(u,v) &= \mathrm{rect}\left[\frac{u}{a_w}\right] * \sum_{n=-\infty}^{\infty}\delta(u-n\cdot d)\\ &= \sum_{n=-\infty}^{\infty}\mathrm{rect}\left[\frac{u-n\cdot d}{a_w}\right], \end{aligned} \tag{4}$$

where $\delta(u)$ denotes the Dirac delta function and * the convolution operation. a_w represents the width of the white stripe and $[u,v]$ represents the frequency coordinates. The corresponding Fourier transform scaled to the wavelength λ and the focal length f is

$$\begin{aligned} g(x,y) &= \sum_{n=-\infty}^{\infty}\frac{a_w}{d}\mathrm{sinc}\left(\frac{a_w}{\lambda f}x\right)\cdot\delta(x-nX_0)\\ &= \sum_{n=-\infty}^{\infty}C_n\cdot\delta(x-nX_0). \end{aligned} \tag{5}$$

The physical meaning of the parameter X_0 is the replica separation in the image plane where its amplitude is modulated by a sinc$(\cdot)$ function. Figure 3 shows the transmittance of the Ronchi ruling with its corresponding Fourier transform. For purpose of visualization in Fig. 3(b), the correspondent sinc$(\cdot)$ function was plotted showing the amplitude change obtained by the zeroth order with the $\pm$1st order.

The transmittance obtained in the image plane will be composed of the convolution of the interference pattern with the Ronchi ruling grating diffraction pattern scaled in the λ and the focal length f.

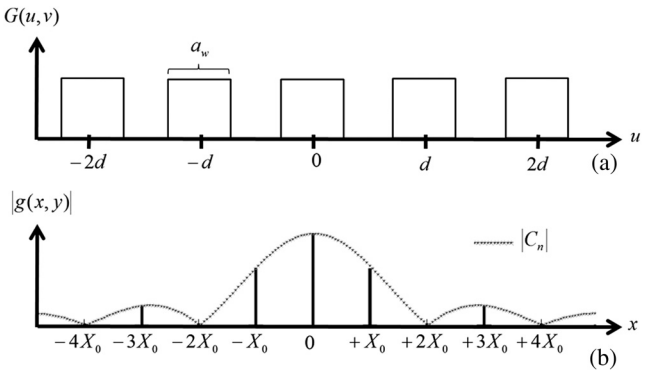

Fig. 3 Transmittance of a Ronchi ruling of spatial period and width of the white strip. The resulting intensity of the diffraction pattern scaled in the wavelength and the focal length results in an amplitude change between orders following a sinc(·) function.

$$I_p(x,y) = g(x,y) * I_\theta(x,y) = \sum_{n=-N}^{N} |C_n| \cdot I_\theta(x - n \cdot X_0, y)$$
$$I_n(x,y) = |C_n|\{1 + \cos[2\theta - \varphi(x,y)]\}, \quad (6)$$

where θ is the angle of the linear polarizer placed over the interference pattern replica and used to introduce the desired phase shift. The term $\varphi(x,y)$ is the phase data map, and C_n is the n-Fourier complex coefficient.

The major drawback of this system is the amplitude interferogram modulation caused by the phase/amplitude gratings.[12] A more detailed study of the replicas obtained by using these techniques can be encountered in Ref. 2. This amplitude modulation can be solved by the implementation of fringe pattern normalization algorithms.[15,16] As a difference from the system previously presented in Ref. 2, in this work, we used only one Ronchi ruling, taking the interference replicas obtained in the $[-1, 0, 1]$ orders and using a fringe pattern normalization algorithm to avoid the interference amplitude difference against the $[-1, 1]$ orders with the [0] order.

3 Temperature Field Measurement

The phase difference $\varphi(x,y)$ between two waves passing through the same point of the phase object, one in the presence of an inhomogeneous medium and the other in the air, is given by[17–20]

$$\varphi(x,y) = \frac{2\pi}{\lambda} \int_0^\Gamma [n(x,y,z) - n_0] \mathrm{d}z, \quad (7)$$

where $n(x,y,z)$ is the refractive index of the medium, n_0 is the refractive index of the air, and Γ is the total length of the medium. In this equation, the optical path difference provides the distortion of the wavefront. In order to evaluate the index refraction difference term, Eq. (7) must be solved. This task can be achieved depending on the structure of the phase object. Taking the thin-flame as a phase object with radial symmetry, the equation of a bright fringe, $N(x) = \varphi(x,y)/2\pi$, of the retrieved interferogram becomes

$$N(x)\lambda = 2\int_x^\infty \frac{f(r)rdr}{\sqrt{r^2 - x^2}}, \quad (8)$$

where $N(x)$ represents the fringe order of the slice to be used to retrieve the refraction index profile. $N(x) = [\varphi(x,y_s)]/2\pi$ and $f(r) = n(r) - n_0$. Equation (8) represents the Abel transform of $f(r)$, and the index of refraction difference is retrieved by using Abel transform inversion techniques.[21] By inverting Eq. (8), we are able to calculate the position dependent index of refraction. Taking into account the Gladstone–Dale relation, $(T) = 1 + K\rho$, expressed under ideal gas assumption, $\rho = p/RT$, we are able to retrieve the temperature profile as

$$T(x,y) = \frac{P}{\left(\rho_{\mathrm{ref}} + \frac{f(x,y)}{K_{G-D}}\right)R}, \quad (9)$$

taking air as a reference at $T = 15$°C with a pressure $P = 101325\ \mathrm{N/m^2}$, $\rho_{\mathrm{ref}} = 1.225$, $R = 287\ \mathrm{J/kg\,K}$ as the specific gas constant, and $K_{G-D} = 0.226 \times 10^{-3}\ \mathrm{m^3/Kg}$ as the Gladstone–Dale constant at $\lambda = 632.8$ nm.[22] Several studies have concluded that the assumption of air is sufficient for premixed flames as a sample, but in a more strictly manner, the Gladstone–Dale and specific gas constants need to be taken into account for specific local component distribution, not in the scope of this work.[23–25]

4 Experimental Setup of the Temperature Field Measurement

The proposed system is based on a PMI coupled to a 4-f system in order to obtain replicas of the interference pattern at the output (Fig. 1). Light from a He-Ne laser at $\lambda = 633$ nm is linearly polarized at 45 deg and divided in amplitude by the beam splitter (BS). Linear polarizers at 0 and 90 deg are placed on the object and reference arms of the PMI, respectively. A quarter-wave plate (QWP) at 45 deg at the output of the interferometer turns linearly polarized light into left-handed and right-handed circularly polarized light, respectively. If we place a linear polarizer at this stage, we could obtain an interference pattern with its phase modulation controlled twice the linear polarizer angle. By placing an amplitude grating with a spatial frequency of 100 lines/mm on the frequency plane of the 4-f system, we are able to obtain replicas with the same capability of phase modulation by placing a linear polarizer angle in each of the replicas obtained (Fig. 2). As a result, we obtain the necessary interference fringe patterns with a relative phase shift in order to retrieve the phase data map properly. After each interferogram is separated from the image, the fringe processing is the same as any other algorithms already implemented in the literature. An He-Ne laser is utilized with a power of 20 mW and $\lambda = 0.633$ μm allowing sufficient illumination intensity to carry out the experiment. The monochromatic camera used is based on a CMOS sensor with 1280×1024 pixels and with a pixel pitch of 6.7 μm. The polarizing filter film that was used is commercially available (Edmund Optics, TechSpecs high contrast linear polarizing film). The size of each polarized film used in each interferogram was 25×25 mm, with its transmission axes oriented at

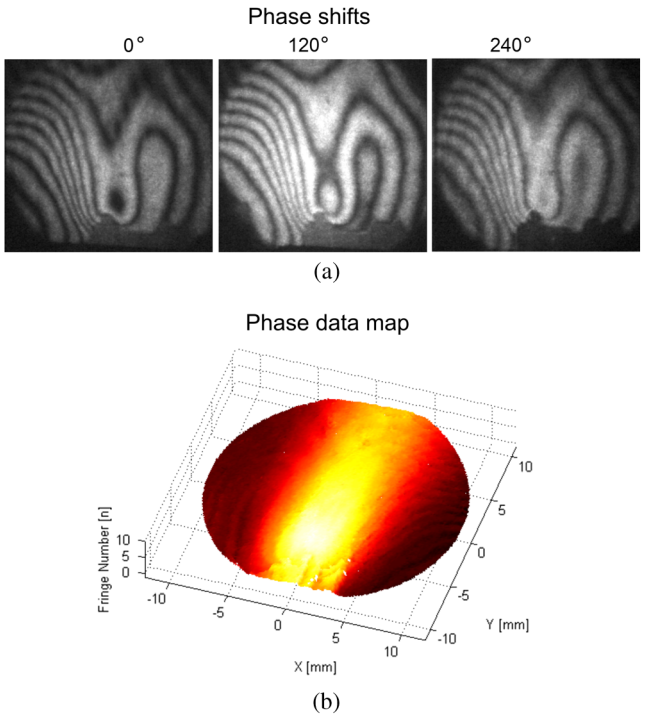

Fig. 4 Experimental results corresponding to the fringe order number obtained by the unwrapped phase map. (a) Three-phase shifted interferograms with amplitude modulation obtained by a single capture used to retrieve the phase data map. (b) By taking a reference phase map, the fringe order localization is directly obtained of the deformed fringe pattern (Video 1, WMV, 0.5 MB) [URL: http://dx.doi.org/10.1117/1.OE.53.11.112202.1].

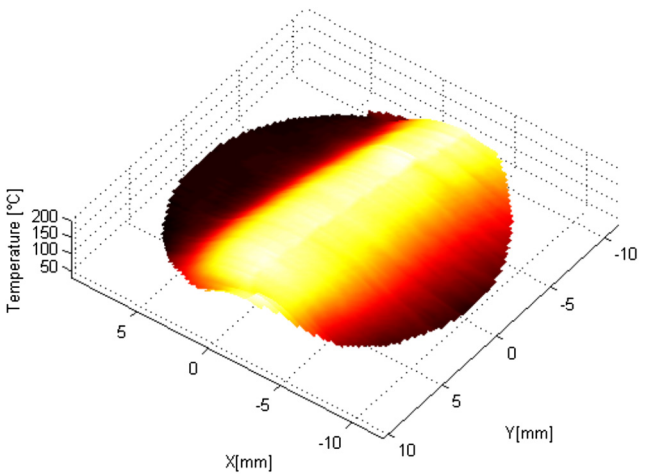

Fig. 5 Temperature profile obtained in a single capture using polarizing phase shifting techniques.

0, 60, and 120 deg. The wrapped phase data map was retrieved using the minimum least square algorithm of three steps,[26] and the unwrapped phase data through the 2-D Goldstein branch cut phase unwrapping algorithm.[27]

A commercial disposable lighter using butane as a fuel was used. The lighter was settled to obtain the minimum flame size possible and prepared to fix the amount of fuel flow during the experiment. The variation observed in the experiment corresponds to the temperature distribution in the region surrounding the flame. Temperature profile measurement was obtained analyzing the dynamic behavior at 8.3 fps in a period of time of 12 s.

Figure 4 presents the three phase-shifted interferograms obtained by a single capture. After a previous calibration procedure,[1] we are capable of retrieving the three phase-shifted interference patterns. By implementing a fringe normalization technique, we are capable of retrieving the phase data map [see Fig. 4(b)]. By taking a reference phase map, the fringe order localization is directly obtained from the deformed fringe pattern, in this case, caused by a thin flame (Video 1).

With the fringe order localization information, we are able to solve the inverse Abel transform [Eq. (8)] and obtain the temperature change occurred by the thin-flame analyzed. Figure 5 shows the typical temperature profile obtained in a single capture.

As the system is able to obtain the dynamic temperature profile in Fig. 6, we present several captures of a dynamic distribution of air temperature that occurred due to environment changes outside of the thin flame (Video 2).

5 Final Remarks

The experimental setup for dynamic temperature field measurements using a single-shot polarization phase shifting technique has been described. This system is able to obtain three phase shifted interferograms in only one shot. Therefore, it is suitable to carry out temporal measurements of temperatures changes occurred outside of a thin flame. The implementations of normalization fringe procedures present the advantage of avoiding the use of phase gratings, and also the advantage of using only three interferograms for the analysis. The system is considerably simpler than previous proposals, showing a suitable alternative to implement in an industrial setting. It is important to note that for this work a polarization change related to the component's temperature variation were not encountered. In order to apply this system for higher temperatures, it is strictly necessary the isolation of the sample without losing its polarization characteristics of the object beam for correct implementations.

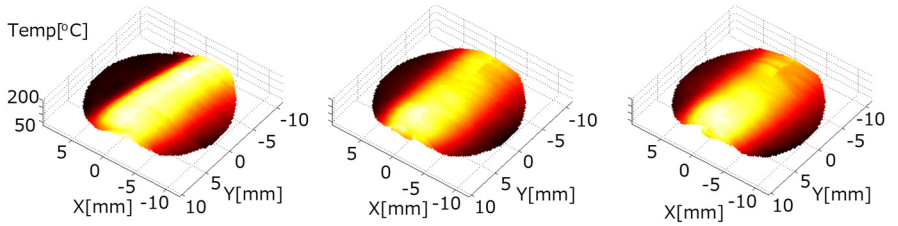

Fig. 6 Temperature phase profiles varying in time (representative frames) (Video 2, WMV, 0.5 MB). [URL: http://dx.doi.org/10.1117/1.OE.53.11.112202.2].

Acknowledgments

Authors thank M. A. Ruiz (CIO), Boaz Jessie Jackin (Utsunomiya Univ. CORE), and Barry Cense (Utsunomiya Univ. CORE) for their contribution in proofreading the manuscript. The authors gratefully acknowledge the research support from the CONACYT under grant 180449. D-I Serrano-García is currently occupying a position as a visiting researcher at Utsunomiya University in the Center for Optical Research & Education (CORE). D-I Serrano-Garcia is very grateful to CONACYT for the graduate scholarship granted (234454-227470/31458) and expresses sincere appreciation to Geliztle for the support provided. N.-I. Toto-Arellano expresses sincere appreciation to Luisa, Miguel, and Damian for the support provided, and to "Programa de Mejoramiento del Profesorado" (PROMEP) for Grant UTTGO-PTC-016.

References

1. N. I. Toto-Arellano et al., "4D profile of phase objects through the use of a simultaneous phase shifting quasi-common path interferometer," *J. Opt.* **13**(11), 115502 (2011).
2. N. I. Toto-Arellano et al., "Slope measurement of a phase object using a polarizing phase-shifting high-frequency Ronchi grating interferometer," *Appl. Opt.* **49**(33), 6402–6408 (2010).
3. D. I. Serrano-García et al., "Radial slope measurement of dynamic transparent samples," *J. Opt.* **14**(4), 045706 (2012).
4. J. E. Millerd et al., "Pixelated phase-mask dynamic interferometer," *Proc. SPIE* **5531**, 304–314 (2004).
5. M. Servin and J. C. Estrada, "Error-free demodulation of pixelated carrier frequency interferograms," *Opt. Express* **18**(17), 18492–18497 (2010).
6. J. M. Padilla, M. Servin, and J. C. Estrada, "Synchronous phase-demodulation and harmonic rejection of 9-step pixelated dynamic interferograms," *Opt. Express* **20**(11), 11734–11739 (2012).
7. S. Equis, R. Schnabel, and P. Jacquot, "Snap-shot profilometry with the Empirical Mode Decomposition and a 3-layer color sensor," *Opt. Exp.* **19**(2), 1284–1290 (2011).
8. J. M. Desse, P. Picart, and P. Tankam, "Digital three-color holographic interferometry for flow analysis," *Opt. Exp.* **16**(8), 5471–5480 (2008).
9. M. W. Kudenov et al., "Spatial heterodyne interferometry with polarization gratings," *Opt. Lett.* **37**(21), 4413–4415 (2012).
10. V. Rosso et al., "Almost-common path interferometer using the separation of polarization states for digital phase-shifting shearography," *Opt. Eng.* **46**(10), 105601 (2007).
11. P. Blain et al., "Combining shearography and interferometric fringe projection in a single device for complete control of industrial applications," *Opt. Eng.* **52**(8), 084102 (2013).
12. N. I. Toto-Arellano et al., "Phase shifts in the Fourier spectra of phase gratings and phase grids: an application for one-shot phase-shifting interferometry," *Opt. Express* **16**(23), 19330–19341 (2008).
13. O. Bryngdahl, "Polarization-type interference-fringe shifter," *J. Opt. Soc. Am* **62**(3), 462–464 (1972).
14. H. J. Okoomian, "A two-beam polarization technique to measure optical phase," *Appl. Opt.* **8**(11), 2363–2365 (1969)
15. J. A. Quiroga, J. A. Gómez-Pedrero, and A. García-Botella, "Algorithm for fringe pattern normalization," *Opt. Commun.* **197**(1–3), 43–51 (2001).
16. J. A. Quiroga and M. Servín, "Isotropic n-dimensional fringe pattern normalizacion," *Opt. Commun.* **224**(4–6), 221–227 (2003).
17. C. M. Vest, *Holographic Interferometry*, John Wiley and Sons, New York (1979).
18. D. P. Correia, P. Ferrão, and A. Caldeira-Pires, "Advanced 3D Emission Tomography Flame Temperature Sensor," *Combustion Sci. Technol.* **163**(1) (2001).
19. C. Shakher and A. K. Nirala, "A review on refractive index and temperature profile measurements using laser-based interferometric techniques," *Opt. Lasers Eng.* **31**(6) (1999).
20. S. Sharma, G. Sheoran, and C. Shakher, "Investigation of temperature and temperature profile in axisymmetric flame of butane torch burner using digital holographic interferometry," *Opt. Lasers Eng.* **50**(10) (2012).
21. E. Ampem-Lassen et al., "Refractive index profiling of axially symmetric optical fibers: a new technique," *Opt. Express* **13**(9), 3277–3282 (2005).
22. T.E. Walsh and K.D. Kihm, "Tomographic deconvolution of laser speckle photography for axisymmetric flame temperature measurement," *J. Flow Visual. Image Process.* **2**(3), 299–310 (1995).
23. K. D. Kihm, "Laser speckle photography technique applied for heat and mass transfer problems," *Adv. Heat Transfer* **30**, 255–311 (1997).
24. Z. Jinrong et al., "Study on the measurement of temperature field using laserholographic interferometry," *Energy* **5**(1), 120–124 (2011).
25. J. A. Qi et al., "Temperature-field measurements of a premixed butane/air circular impinging-flame using reference-beam interferometry," *Appl. Energy* **83**(12), 1307–1316 (2006).
26. M. Servin, J. C. Estrada, and J. A. Quiroga, "The general theory of phase shifting algorithms," *Opt. Express* **17**(24), 21867–21881 (2009).
27. D. C. Ghiglia and M. D. Pritt, *Two-Dimensional Phase Unwrapping: Theory, Algorithms and Software*, Wiley-Interscience, New York (1998).

David Ignacio Serrano-García received his bachelor's degree from the Monterrey Institute of Technology and Higher Education in physical engineering in 2008 and his master's degree in optics in 2010 from the Centro de Investigaciones en Optical A.C. in Leon, Guanajuato, Mexico. He is currently working toward his PhD in the same institution. His main research involves optical metrology and polarization phase shifting techniques applied to single-shot interferometry measurements.

Amalia Martínez-García received her PhD in optics at Centro de Investigaciones en Óptica, Mexico (CIO). She was a research scientist at Centro de Investigación Científica y de Educación Superior de Ensenada. Currently, she is a full-time researcher at CIO and member level II of the National System of Researchers, Mexico. She is the vice-president of the Mexican Academy of Optics during 2013–2014 and elected president 2015–2016. Her research area is in optical metrology.

Noel-Ivan Toto-Arellano received his BS degree in physical sciences at Universidad Veracruzana, México, his MSc in optical sciences from Benemerita Universidad de Puebla in 2005, and his PhD in optical sciences from the same institution in 2008. He did two postdoctoral internships at CIO. He currently holds a research professor position in Universidad Tecnológica de Tulancingo, Hidalgo, México, supporting the creation of a photonics engineering program at the same university.

Yukitoshi Otani is a professor at the Center for Optical Research and Education, Utsunomiya University, Japan. He received his doctorate from the University of Tokyo in 1995. He was an associate professor at Tokyo University of Agriculture and Technology until 2010 and visiting professor at the College of Optical Sciences, the University of Arizona, from 2004 to 2005. He is a fellow of SPIE since 2010.